

# The Stomata of the Katanin Mutants, *Fra2*, *Lue1* and *Bot1* †

Dafni Paraskevopoulou, Nikolaos Anezakis, Eleni Giannoutsou, Penelope Sotiriou and Ioannis-Dimosthenis S. Adamakis \*

Department of Botany, Faculty of Biology, National and Kapodistrian University of Athens, Greece

\* Correspondence: iadamaki@biol.uoa.gr; Tel.: +30-201-7274653

† Presented at the 1st International Electronic Conference on Plant Science, 1–15 December 2020; Available online: <https://iecps2020.sciforum.net/>.

Published: 1 December 2020

**Abstract:** Katanin, is a microtubule severing protein that orchestrates microtubule organization throughout the plant cell cycle. Taking into consideration the role of the microtubule cytoskeleton in the stomatal development, the *Arabidopsis thaliana* katanin mutants, *fra2*, *lue1* and *bot1* were studied to observe how the absence of function of/malfunction of katanin affects stomatal development. Katanin mutants are characterised by less mature stomata and more young stomata and meristemoids forming clusters. The size of the mature stomata differed from col-0, with the katanin mutants having shorter guard cells and pores as well as smaller pore aperture. Also a unique type of cells was observed in the *fra2* mutant, the persistent guard mother cells (GMC's), where the GMC persisted and did not divide symmetrically to form a stoma. Another, rather significant observation was that, the cell walls of some epidermal cells in the mutants appeared to be incomplete. As far as the cell wall matrix components distribution is concerned, callose did not display significant differences compared to col-0 while pectins and hemicelluloses were differentially dispersed. Microtubules in cytokinetic GMCs were long, bended and connected to the nuclei, while microtubule arrays in katanin mutant leaf epidermis were aberrant and stomatal complexes had astral microtubule arrays as it was observed in the wild type. In conclusion, the malfunction of katanin appears to affect the development of stomata in the epidermis of young leaf in *Arabidopsis thaliana*, affecting not only stomatal patterning, since the one-cell spacing rule was compromised, but also the morphology of the stomatal complexes. The cell wall-matrix appears altered in the katanin mutants possible affecting the function of the stomata since katanin mutant stomata had a reduced pore aperture.

**Keywords:** katanin; *fra2*; *lue1*; *bot1*; stomata; callose; pectins

---

## 1. Introduction

The developmental process by which stomata form, consists of a series of cellular differentiations and divisions, where a subset of protodermal cells eventually differentiates into meristemoid mother cells (MMC) [1,2]. An MMC divides asymmetrically to produce a small triangular cell called a meristemoid and a larger cell called a stomatal-lineage ground cell (SLGC). An SLGC can terminally differentiate into a lobed pavement cell (PC). Sometimes, a second asymmetric spacing division occurs to produce a satellite meristemoid, which is always placed distal to an existing stoma or precursor. The meristemoid transits into a guard cell mother cell (GCM) and symmetrically divides resulting in two guard cells that form the stoma [2]. This series of events is a tightly genetically controlled process [3] thus, stomatal distribution is not random and it follows a certain rule, the one epidermal cell spacing rule which means that stomata must always be separated by at least one pavement cell [4].

Katanin, especially the p60 subunit, functions as a microtubule severing protein [5]. *Arabidopsis thaliana* mutants of the p60 subunit that were characterized are: *bot1*, *fra2*, *erh3*, *lue1*, *katanin*, all allelic to each other. All of the above are semi-dwarf and thick plants, with all of their organs being shorter than those of the wild type (Col-0) [6]. These irregularities in the morphology of mutants, especially

in the root and shoot, were attributed to the failure of cortical microtubules to follow a uniform transverse orientation in elongating cells. Consequently, as cortical microtubules provide the pattern for cellulose microfibril deposition, defective cortical microtubule arrangement results in aberrant cellulose microfibril orientation in the expanding cell wall. This, in turn, favors a rather isotropic cell growth, responsible for the characteristic phenotype of the above mutants [6–8].

The kidney-shaped *A.thaliana* guard cells contain an unusual array of radially-oriented microtubules that converge near the central rim of the stomatal pore. The assembly of this array starts just after GMC division. This array becomes prominent before any thickenings in the new wall can be detected, and the locations of the array foci predict where pore wall swelling will occur later [9]. Therefore, taking into consideration the characteristics of the katanin mutants and the distribution of the microtubule cytoskeleton during stomatal development [9], the katanin mutants *fra2*, *lue1*, and *bot1* were studied to observe how the absence of function /malfunction of katanin affects stomatal development. The number of stomata (mature and young) as well as the number of meristemoids was quantified per surface unit in cotyledons of 7-day old plants. Furthermore, the length and the width of the guard cells were measured, as well as the pore length and pore aperture. Next, the distribution of cell-wall components on the stomatal cell wall-matrix was studied using aniline blue for callose staining and immunofluorescence to observe various pectins and hemicelluloses. Finally, the possible changes in microtubule organization were investigated in a GFP-TUA *lue1* expressing line.

## 2. Experiments

### 2.1. Plant Material

This study was carried out in young cotyledons of *Arabidopsis thaliana* grown in ½ strength MS growth medium for 7 days. All of the seeds used in this study were purchased by NASC.

### 2.2. Preparation of semithin sections and Toluidin Blue O staining

Small leaf pieces fixed in 2% (*w/v*) PFA and 0.1% (*v/v*) glutaraldehyde in PEM at 4 °C for 1.5 h. The specimens were washed in the same buffer and dehydrated in a graded ethanol series (10–90%) diluted in distilled water and three times in absolute ethanol for 30 min (each step) at 0 °C. The material was post-fixed with 0.25% (*w/v*) osmium tetroxide added to the 30% ethanol step for 2 h. The material was infiltrated with LR White (LRW) (Sigma) acrylic resin diluted in ethanol, in 10% steps to 100% (1 h in each), at 4 °C and with pure resin overnight. The samples were embedded in gelatin capsules filled with LRW resin and polymerized at 60 °C for 48 h. The samples were stained with Toluidin O in order to be observed in light microscopy.[10]

### 2.3. Callose Localization

Callose in living stomatal complexes was localized in paradermal hand-made leaf sections stained with 0.05% (*w/v*) aniline blue (Sigma, C.I. 42725) in 0.07 M K<sub>2</sub>HPO<sub>4</sub> buffer, pH 8.5 [11]. Sections remained in aniline blue solution during observation at the epifluorescent microscope.

### 2.4. Immunolocalization of Pectins, Hemicelluloses and Microtubules

For immunolabeling of LM20- (homogalacturonans displaying a high degree of methylesterification), JIM5- (homogalacturonans displaying a lower degree of methylesterification), and 2F4 (demethylesterified homogalacturonans interconnected with calcium bridges), as well as LM25 and LM15 (xyloglucans)- HG epitopes in paradermal hand-made leaf sections the following protocol was performed [12]. The specimens were fixed in 8% (*w/v*) paraformaldehyde (PFA) in PEM buffer (50 mM PIPES [piperazine-N,N'-bis(2-ethanesulphonic acid)], 5 mM EGTA, 5 mM MgSO<sub>4</sub>, pH 6.8) for 45 min. Then, the leaf sections were washed three times with PEM for 15 min and treated with 1% (*w/v*) cellulase in PEM, pH 5.6, for 60 min. After washing with PEM, the sections were extracted with 0.5% (*v/v*) Triton X-100 and 2% (*v/v*) dimethylsulphoxide (DMSO) in Phosphate Buffer Saline

(PBS) for 20 min and transferred to PBS containing 2% (*w/v*) BSA for 1 h. The sections were incubated overnight with the anti-callose antibody (Biosupplies, Parkville, Australia) diluted 1:40 in PBS containing 2% (*w/v*) BSA, and rinsed three times with PBS, for 15 min each time. They were transferred to PBS containing 2% (*w/v*) BSA and incubated for 1 h at 37 °C in FITC anti-mouse IgG (Sigma), washed with PBS and mounted with a mixture of glycerol/PBS (2:1 *v/v*) containing 0.5% (*w/v*) p-phenylenediamine (anti-fade medium). LM20, JIM5 and 2F4 (Plant Probes, Leeds, UK) were used as primary antibodies and FITC-conjugated anti-rat IgG (Sigma) as secondary antibody in all cases. The various categories of HGs recognized by LM20, JIM5 and 2F4 antibodies are thoroughly described at the end of the Introduction section. All antibodies were diluted 1:40 in PBS that contained 2% (*w/v*) BSA except for 2F4 and its secondary antibody, which were diluted 1:40 in T/Ca/S buffer (Tris-HCl 20 mM pH 8.2, CaCl<sub>2</sub> 0.5 mM, NaCl 150 mM). During the immunolabeling procedure with 2F4 antibody, the sections were washed with T/Ca/S buffer (for details see Plant Probes leaflet). For microtubules immunolocalisation, YOL antibody (anti-TUA) has been used as primary antibody, followed by anti-rat FITC as secondary antibody.

#### 2.4. Observation and Photography

The specimens were examined with a Zeiss Axioplan microscope equipped with a UV source, a Differential Interference Contrast (DIC) optical system, and a Zeiss Axiocam MRc5 digital camera. Two filter sets were used for the specimens observation: a filter set provided with exciter solid glass filter 365 nm and barrier long-wave pass band filter 420 nm, and another set provided with exciter pass band filter 450–490 nm and barrier pass band filter 515–565 nm. Series of paradermal optical sections have been studied, to ascertain the distribution of the examined cell wall materials along the whole surface of the cell walls. At least three independent experiments have been conducted for callose and LM20-, JIM5- and 2F4- HG epitopes localization in *Arabidopsis thaliana* stomatal complexes. Furthermore, more than twenty sections were examined in every experiment. All samples were checked for UV autofluorescence using the above filters. GFP-TUA lines were observed under a Zeiss Observer.Z1 microscope equipped with the LSM 780 confocal laser scanning system, while image acquisition was done with the ZEN 2011 software [13].

### 3. Results

#### 3.1. Stomatal Development and Stomatal Characteristics in Katanin Mutants

Katanin mutant's stomata had shorter guard cells and pores as well as smaller pore aperture (Figure 1 A,B) while the width of the guard cell was similar with the wild type (Figure 1A,B). Also katanin mutants bore less mature stomata but more young stomata and meristemoids (Figure 1 C,D.) with *fra2* to exhibit more striking differences when compared with the Col-0 (Figure 1D). More importantly katanin mutants displayed abnormalities regarding the stomata distribution, with the meristemoids and the mature stomata to be in contact forming clusters (Figures 2 and 3). A unique type of cells was observed in the *fra2* mutant, the persistent GMC's, where guard mother cells persisted and did not divide symmetrically to form a stoma but at the same time they had guard cell characteristics/properties (Figure 3F).

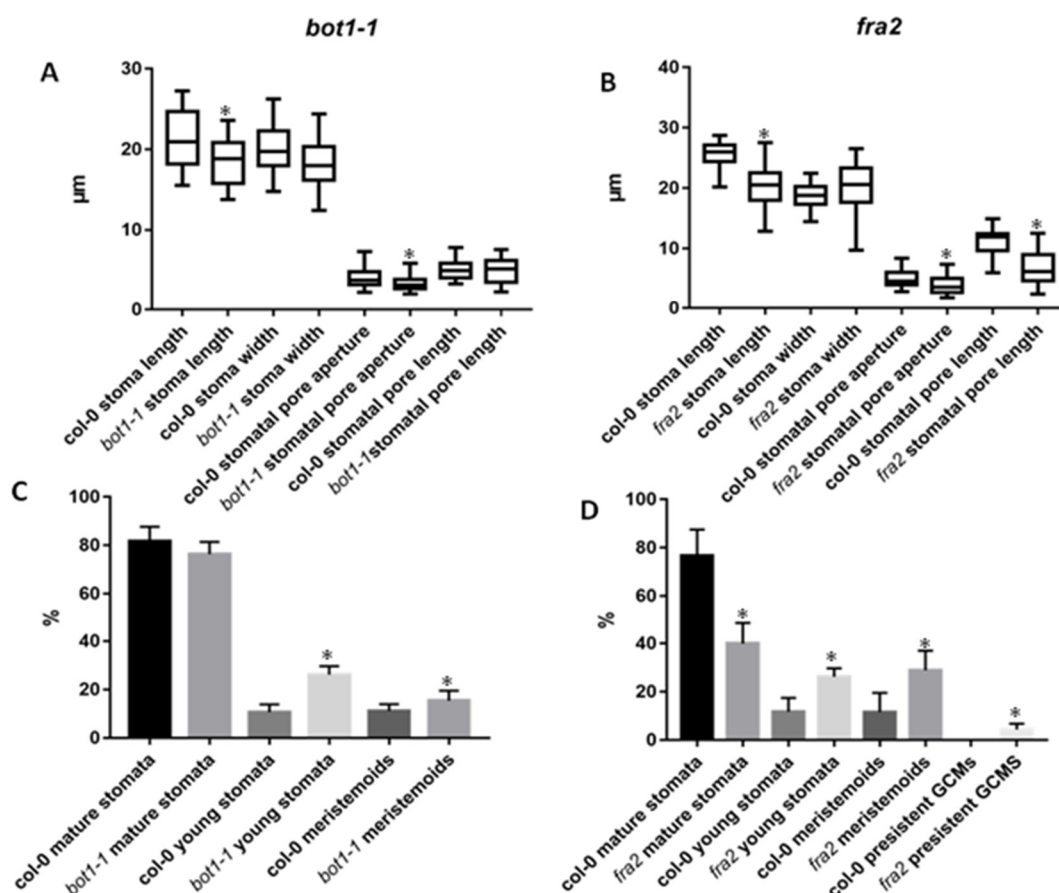


**Figure 1.** Diagrams showing either the characteristics of the morphology of the developing stomata (A,B) or the stages of the stomatal development (C,D) in Col-0, *bot1* and *fra2* cotyledones. Asterisks show statistical significance set at  $p < 0.05$ .

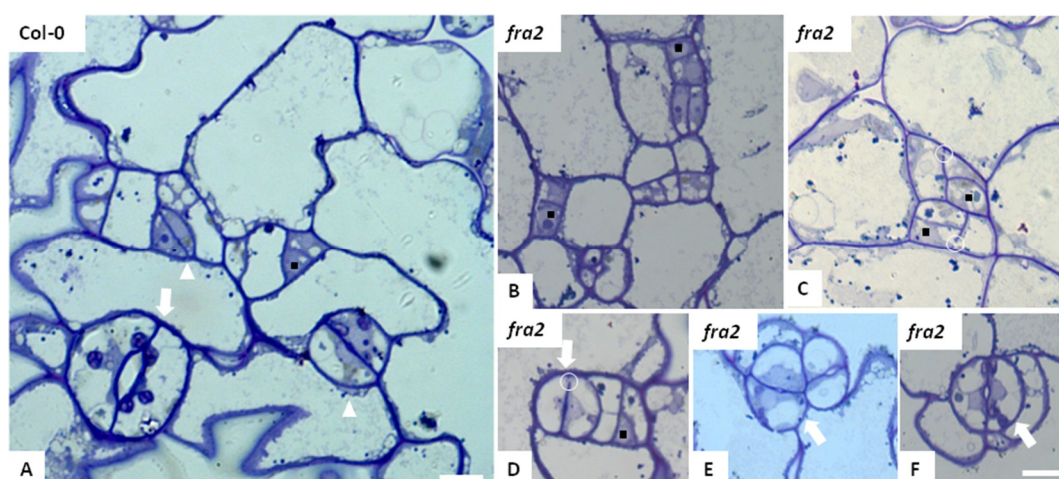


**Figure 2.** Semithin sections of chemically fixed and embedded in plastic cotyledones of Col-0 (A) and *fra2* (B–F) stained with toluidin blue O. Col-0 epidermis (A) had a typical appearance with mature stomata (arrows), young stomata (arrowheads) and meristemoids (black squares) being orderly arranged, obeying the one epidermal spacing rule. In *fra2* the meristemoids appeared in clusters (B,C) while mature stomata (F) were commonly found in pairs in close contact (D,E). In some cases incomplete cell walls were visible (circles in C and D). Bars: 20 µm in A, 20 µm in B–F.

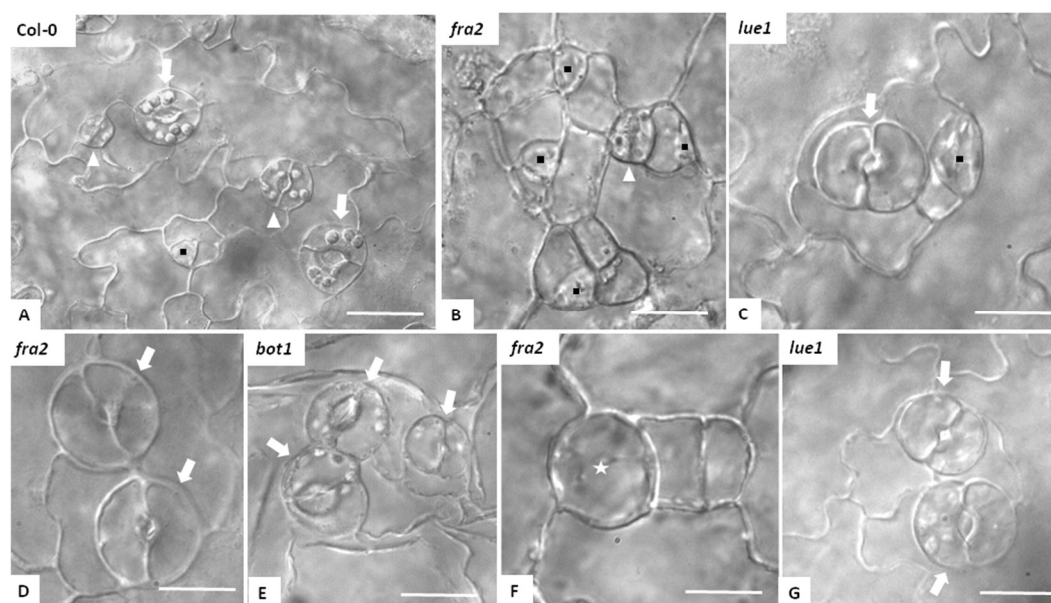


**Figure 3.** DIC microscope images of epidermis of cotyledones of Col-0 (A), *fra2* (B,D,F), *bot1* (E) and *lue1* (C,G). In Col-0 no defects can be observed with the mature, young stomata and the meristemoid cells to obey the one epidermal spacing rule. In contrast in katanin mutants's epidermis either meristemoid clusters (B) or mature stomata pairs in contact could be observed (C–E,G). In *fra2* persistent GMCs could be also observed (star in F). Bars: 20  $\mu$ m.

### 3.2. Stomatal Patterning in Katanin Mutants

The stomatal complexes of *Arabidopsis thaliana* are comprised of two guard cells surrounded by a number of epidermal cells that can be smaller than the usual epidermal cells and are the result of a meristemoid cell being divided more than once before differentiating into a GMC (anisocytic complexes) (Figure 2A). Whereas, when this meristemoid is divided only once or not at all, the epidermal cells are of regular size (nonanisocytic complexes). In Figure 2, in *fra2* mutants, the initial meristemoid cell continues to divide asymmetrically, giving rise to a number of small meristemoid cells, in close contact to each other (Figure 2B,C). This eventually results in the formation of stomatal complexes appearing in clusters, when cell differentiation is complete (Figure 2E,F). Local thickenings on the cell wall regions lined by the preprophase microtubule band are characteristic at the guard cell mother cells (GMCs) of *A. thaliana*, also observed in Leguminosae species. As a result, the junction of the dorsal cell walls of the young GCs appear thickened, while the ventral wall end is tightly connected to these thickenings (white arrow and arrowhead in Figure 2A). In *fra2* mutants, these cell wall thickenings of the dorsal walls at the junction sites, may not have been completely formed due to the microtubules inability to be accurately placed (Figure 2E,F). Another significant observation was the incomplete cell walls observed after chemical fixation of the tissue (circles in Figure 2C,D), resulting in cells that were connected through the gaps that were created (Figure 2B–F).

In Figure 3, the increased number of meristemoids in *fra2* mutants is clearly observed (Figure 3B), as well as the clustering of the stomatal complexes (Figure 3C–E), where it is obvious that the one cell spacing rule is compromised. Another significant observation is that, in many GMCs, the symmetrical division is absent. These cells grow in size and differentiate without becoming guard cells. These cells, observed in Figure 3F (asterisk) are called persistent GMCs.

### 3.3. Callose Deposition in *Fra2*, *Lue1* and *Bot1* Mutants

Callose deposition in katanin mutants (Figure 4C–F) did not display significant differences compared to Col-0 (Figure 4A,B). Aniline blue staining was prominent in young cell plates (arrowheads in Figure 4A,C–E) while in the mature stomata a strong staining in the polar ventral cell

wall ends has been observed (white arrows in Figure 4A–F) even at stomata in close contact (Figure 4C–F).

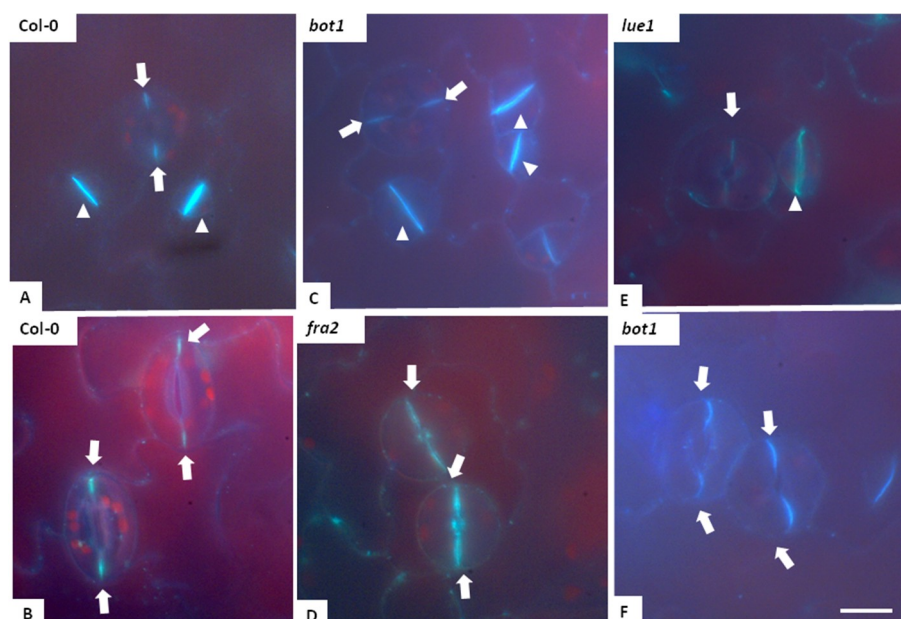


**Figure 4.** Aniline staining in Col-0 (A,B) *fra2* (D), *lue1* (E) and *bot1* (I–L) epidermis of cotyledons. Arrows point to cell wall thickenings at the junction sites of the dorsal cell walls, while arrowheads point to the newly formed cell walls. No significant differences can be observed between Col-0 and the katanin mutants. Bar: 20  $\mu$ m.

### 3.4. Hemicellulose and Pectin Deposition in Stomatal Complexes of *fra2* and *Bot1* Mutants

Cell wall-matrix components distribution is altered in the mature stomata of katanin mutants (Figures 5 and 6). As far as hemicelluloses are concerned, LM25 and LM15 (xyloglucans) epitopes in Col-0 stomata (Figure 1A–C) were strongly deposited at the cell wall thickenings of the dorsal cell wall junctions and weakly found at the polar ventral cell wall ends (brackets in Figure 1C). Katanin mutants stomata exhibited either a signal covering a smaller area of the dorsal cell wall junctions (Figure 1G,K) or were ectopically placed in the stomata periphery (Figure 5E,I). In mature Col-0 stomata, the LM20-, and JIM5-, homogalacturonan (HG) epitopes were mainly found at the cell wall thickenings of the dorsal cell wall junctions, at the polar ventral cell wall ends and at the base the stomatal pore ledges (Figure 6C,D). In the latter, the presence of LM20-HG epitope was intense in Col-0 (Figure 6A). The 2F4-HG epitope showed a prominent distribution at the dorsal cell wall of the guard cells (Figure 6E) in Col-0 while in katanin mutants intense signal was observed in the dorsal cell wall junctions (Figure 6 K,L,Q). LM20-and JIM5-HG in katanin mutants were distributed boardly in the dorsal cell walls of the guard cells at the stomata periphery (Figure 6 G–I,M,O).

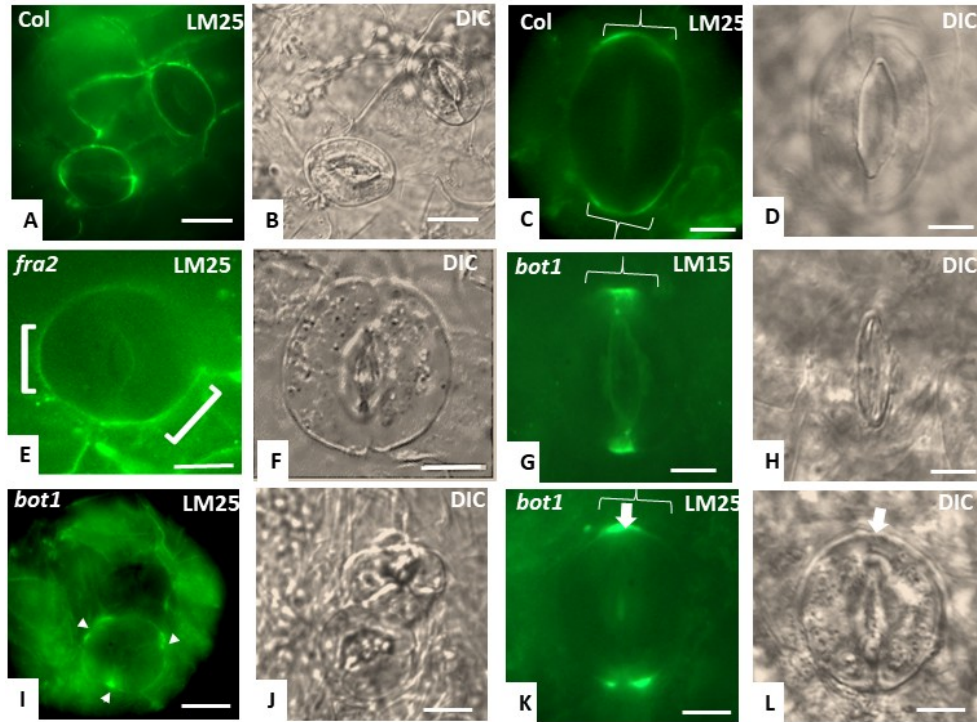


**Figure 5.** Mature *A. thaliana* stomata following LM25 and LM15 hemicelluloses epitope localization. All pictures taken from paradermal hand-made leaf sections. (A,C,E,G,I,K) Surface optical section of stomata as appears after LM25 (A,C,E,I,K) and LM15 antibody immunolabeling (G) and as seen by DIC optics (B,D,F,H,J,L). Brackets in E show immunodetection at the dorsal cell walls, while brackets in C, G and K and arrow in K point to the cell wall thickenings at the junction sites of the dorsal cell walls. Bar: 20  $\mu$ m.

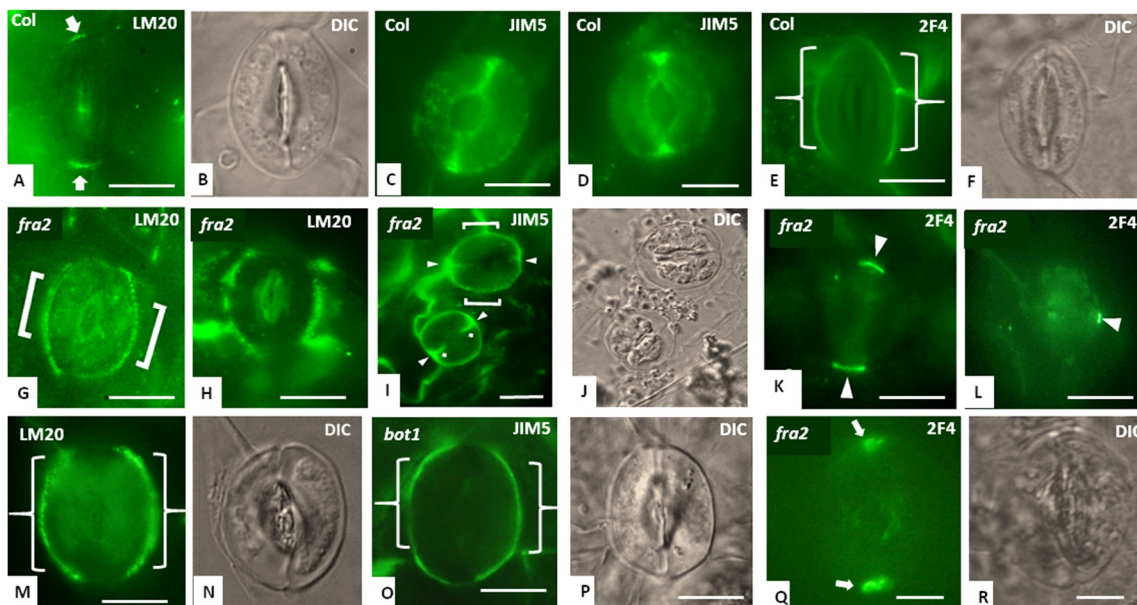


**Figure 6.** Mature *A. thaliana* stomata following LM20, JIM5 and 2F4 homogalacturonans epitope localization. All pictures taken from paradermal hand-made leaf sections. Localization of the LM20-HG epitope in surface optical sections of Col (A), *fra2* (G,H) and *bot1* (M) and as seen in DIC optics (B,N) respectively. Localization of the JIM5-HG epitope in surface optical sections of Col (C,D), *fra2* (I) and *bot1* (O) and as seen in DIC optics (J,P) respectively. Localization of the 2F4 epitope in surface optical sections of Col (E), *fra2* (K,L) and as seen in DIC optics (F,R) respectively. Brackets in (E,G,M,O) show immunodetection at the dorsal cell walls, while arrows point to cell wall thickenings. Bar: 20  $\mu$ m.

### 3.5. Microtubules in *Fra2* and *Bot1* Mutants

Microtubules in dividing cells of *fra2* (Figure 7G) were long, bended and connected to the nuclei of the newly developed/daughter cells when compared with Col-0 (Figure 7E) while in the *lue1* mutant, even though microtubule arrays on the leaf epidermis were aberrant (Figure 7C), stomatal complexes had astral microtubule arrays as those observed in the wild type (Figure 7B,D). The prophase spindle of the *fra2* mutants cotyledone diving cells were multi-polar (arrowhead in Figure 7F) with aberrant prophase microtubule zone (Figure 7F).

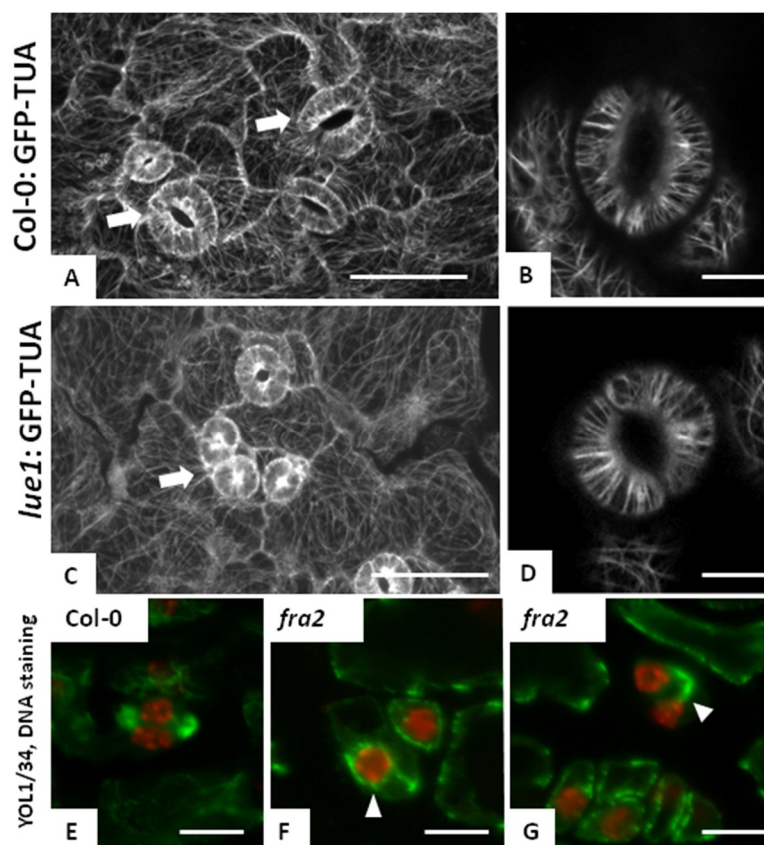


**Figure 7.** Microtubules observed at Col-0, *lue1* and *fra2* katanin mutants. In (A–D), GFP-TUA constructs were observed at CLSM microscopy. In (E–G), microtubules immunodetection was performed and DNA staining followed at hand made fresh leaves sections. Arrows point to stomatal complexes. Bar: 20 μm.

## 4. Discussion

Up until now katanin protein defects in the leaf epidermis have been linked: (a) With the bulky and distorted longitudinally arranged cells of the *dgl1* rice katanin mutant which had crescent-, triangle-, trapezoid-, or circular-shaped cells contrast to the wild type, which developed only rectangular cells [14]; (b) with the disturbed linear arrangement of the stomatal cells in the *dgl1* mutant, [14], and (c) with, the defective pavement epidermal *lue1* cells and the reduced stomatal length in *lue1* [15]. The present study consolidated and extended the above results with the stomatal development to appear altered in both *fra2* and *bot1* mutants as well (Figures 2 and 3). Katanin defects not only affected the stomatal morphology but altered the distribution/development of mature, young and meristemoids (Figures 1 and 3). These results suggest that the role of katanin protein in stomatal cell differentiation and development is also pronounced as it has been reported for other cell types [7,8].

The presence of numerous double stomata in the above mutants could be due to defects in either division plane determination, or cell plate guidance to the predetermined division site, as it has been



reported in root cells [7]. Failure of cytokinesis to occur at the proper division plane may be due to defects in preprophase band positioning, to the absence of identity factors from the cortical division site, or to lack of guidance of the growing cell plate to the cortical division site [16]. An important observation, toward elucidating the above finding, is that in *fra2* meristemoid dividing cells, defected preprophase bands and multipolar prophase spindles were present (Figure 7). Cytokinesis outside the proper division plane seems likely to be the outcome of prophase spindle multipolarity, in which the dominant prophase spindle poles are obliquely arranged on the nuclear surface, metaphase/anaphase spindles acquire oblique orientation, inherited by the phragmoplasts/cell plates as well. Consequently, as cytokinesis proceeds, the cell plate expands away from the predetermined division plane and produces an oblique daughter cell wall and not properly arranged stomata develop (Figures 2 and 3). Moreover, the incomplete cell walls observed (Figure 1) could lead to stomatal lineage determinant factor leakage (e.g., BASL [17]) to meristemoid neighbouring cells causing their re-programming towards the development of stomata, so that stomatal clusters appear (Figure 2).

Another important finding was the altered hemicellulose and HG-epitope distribution occurring in katanin mutant's stomata (Figures 5 and 6). Extending the katanin mutant cell types in which cell wall matrix materials are defectively deposited [18], stomata complexes had a problematic LM25-, LM15- xyloglucan, and LM20, JIM5-, 2F4-HG epitope deposition in the cell wall thickenings in the polar ventral ends and dorsal cell wall junctions indicating that the rigidity of this area is compromised. Rigid stomatal polar ends are important for guard cell function [12,19], which in katanin mutants is disturbed, since a reduced pore aperture was noticed (Figure 1). These cell wall matrix deposition defects could be the outcome of the observed meristemoid preprophase band malformations given that, during preprophase, the polar cell wall thickenings are established [20].

## 5. Conclusions

In conclusion, the malfunction of katanin appears to affect the development of stomata in the epidermis of cotyledones in *Arabidopsis thaliana* considering that we have cases where the one-cell spacing rule is not observed, the cell wall biosynthesis is interrupted and it is possible that the function of the stomata is also affected since katanin mutant stomata had a reduced pore aperture.

**Author Contributions:** E.G., P.S. and I-D.S.A. conceived and designed the experiments; P.S., D.P. and N.A. performed the experiments; E.G. and I-D.S. A. wrote the paper. All of the authors contributed to its finalization. All authors have read and agreed to the published version of the manuscript.

**Acknowledgments:** The present study was supported via funds of the National Kapodistrian University of Athens (Greece).

**Conflicts of Interest:** The authors declare no conflict of interest.

## Abbreviations

The following abbreviations are used in this manuscript:

DIC	diffentiate interphase contrast
GMC	guard mother cells
HG	homogalacturonans
MMC	mereistemoid mother cells
PC	pavement cells
SLGC	stomatal-lineage ground cell

## References

1. Han, S.K.; Torii, K.U. Lineage-specific stem cells, signals and asymmetries during stomatal development. *Development* **2016**, *143*, 1259–1270.
2. Pillitteri, L.J.; Dong, J. Stomatal Development in Arabidopsis. *Arab. Book* **2013**, *11*, e0162.

3. Chater, C.C.C.; Caine, R.S.; Fleming, A.J.; Gray, J.E. Origins and evolution of stomatal development. *Plant Physiol.* **2017**, *174*, 624–638.
4. Zoulias, N.; Harrison, E.L.; Casson, S.A.; Gray, J.E. Molecular control of stomatal development. *Biochem. J.* **2018**, *475*, 441–454.
5. Nithianantham, S.; McNally, F.J.; Al-Bassam, J. Structural basis for disassembly of katanin heterododecamers. *J. Biol. Chem.* **2018**, *293*, 10590–10605.
6. Luptovčiak, I.; Komis, G.; Takáč, T.; Ovečka, M.; Šamaj, J. Katanin: A sword cutting microtubules for cellular, developmental, and physiological purposes. *Front. Plant Sci.* **2017**, *8*, 1982.
7. Panteris, E.; Adamakis, I.-D.S.; Voulgari, G.; Papadopoulou, G. A role for katanin in plant cell division: Microtubule organization in dividing root cells of *fra2* and *lue1* *Arabidopsis thaliana* mutants. *Cytoskeleton* **2011**, *68*, 401–413.
8. Panteris, E.; Adamakis, I.-D.S. Aberrant microtubule organization in dividing root cells of *p60*-katanin mutants. *Plant Signal. Behav.* **2012**, *7*, 16–18.
9. Lucas, J.R.; Nadeau, J.A.; Sack, F.D. Microtubule arrays and *Arabidopsis* stomatal development. *J. Exp. Bot.* **2006**, *57*, 71–79.
10. Moustaka, J.; Panteris, E.; Adamakis, I.-D.S.; Tanou, G.; Giannakoula, A.; Eleftheriou, E.P.; Moustakas, M. High anthocyanin accumulation in poinsettia leaves is accompanied by thylakoid membrane unstacking, acting as a photoprotective mechanism, to prevent ROS formation. *Environ. Exp. Bot.* **2018**, *154*, 44–55.
11. Kohari, M.; Shibuya, N.; Kaku, H. Simultaneous visualization of callose deposition and plasma membrane for live-cell imaging in plants. *Plant Cell Rep.* **2020**, *39*, 1517–1523.
12. Giannoutsou, E.; Sotiriou, P.; Nikolakopoulou, T.L.; Galatis, B.; Apostolakos, P. Callose and homogalacturonan epitope distribution in stomatal complexes of *Zea mays* and *Vigna sinensis*. *Protoplasma* **2019**, *257*, 141–156.
13. Adamakis, I.D.S.; Panteris, E.; Eleftheriou, E.P. Tungsten disrupts root growth in *Arabidopsis thaliana* by PIN targeting. *J. Plant Physiol.* **2014**, *171*, 1174–1187.
14. Komorison, M.; Ueguchi-Tanaka, M.; Aichi, I.; Hasegawa, Y.; Ashikari, M.; Kitano, H.; Matsuoka, M.; Sazuka, T. Analysis of the rice mutant dwarf and gladius leaf 1. Aberrant katanin-mediated microtubule organization causes up-regulation of gibberellin biosynthetic genes independently of gibberellin signaling. *Plant Physiol.* **2005**, *138*, 1982–1993.
15. Bouquin, T.; Mattsson, O.; Næsted, H.; Foster, R.; Mundy, J. The *Arabidopsis lue1* mutant defines a katanin *p60* ortholog involved in hormonal control of microtubule orientation during cell growth. *J. Cell Sci.* **2003**, *116*, 791–801.
16. Van Damme, D. Division plane determination during plant somatic cytokinesis. *Curr. Opin. Plant Biol.* **2009**, *12*, 745–751.
17. Muroyama, A.; Gong, Y.; Bergmann, D.C. Opposing, Polarity-Driven Nuclear Migrations Underpin Asymmetric Divisions to Pattern *Arabidopsis* Stomata. *Curr. Biol.* **2020**, *30*, 4467–4475.e4.
18. Meidani, C.; Ntalli, N.G.; Giannoutsou, E.; Adamakis, I.D.S. Cell wall modifications in giant cells induced by the plant parasitic nematode *meloidogyne incognita* in wild-type (*Col-0*) and the *fra2* *Arabidopsis thaliana* katanin mutant. *Int. J. Mol. Sci.* **2019**, *20*, 5465.
19. Carter, R.; Woolfenden, H.; Baillie, A.; Amsbury, S.; Carroll, S.; Healicon, E.; Sovatzoglou, S.; Braybrook, S.; Gray, J.E.; Hobbs, J.; et al. Stomatal Opening Involves Polar, Not Radial, Stiffening Of Guard Cells. *Curr. Biol.* **2017**, *27*, 2974–2983.e2.
20. Galatis, B.; Apostolakos, P. The role of the cytoskeleton in the morphogenesis and function of stomatal complexes. *New Phytol.* **2004**, *161*, 613–639.

**Publisher's Note:** MDPI stays neutral with regard to jurisdictional claims in published maps and institutional affiliations.



© 2020 by the authors. Submitted for possible open access publication under the terms and conditions of the Creative Commons Attribution (CC BY) license (<http://creativecommons.org/licenses/by/4.0/>).